Remote Detection and Quantification of Methane Emissions Based on Hyperspectral Data Analysis

Mariusz Kastek, Andrzej Ligienza
TechnoVis Sp. z o.o., Towarowa 20 B, 10-417 Olsztyn

Tomasz Sosnowski
Wojskowa Akademia Techniczna, Instytut Optoelektroniki, ul. gen. S. Kaliskiego 2, 00-908 Warszawa

Jadwiga Holewa-Rataj, Mateusz Rataj
Instytut Nafty i Gazu – Państwowy Instytut Badawczy, ul. Lubicz 25A, 31-503 Kraków

Anna Timofiejczuk, Sebastian Rzydzik
Politechnika Śląska, Wydział Mechaniczny Technologiczny, ul. Akademicka 2A, 44-100 Gliwice

Abstract: Measurement of methane emissions from leaks occurring on the territorially extensive network of transmission gas grid is a topical issue and highly desirable from the point of view of safety and reducing methane emissions into the atmosphere. Remote detection of methane is a problem whose technical solution is based on several types of optoelectronic devices, e.g. thermal imaging cameras with sets of optical filters, spectroradiometers, laser systems of the DIAL (DIfferential Absorption Lidar) type. On the other hand, the quantification of emission magnitudes is in most cases realized by spectoradiometric systems. This paper will present a method for analyzing hyperspectral data from an imaging Fourier infrared spectroradiometer. Measurements will be made on a purpose-built bench simulating methane emissions from a transmission network. Data obtained from ground level under different atmospheric conditions will be presented, together with the results of their analysis for different methane emissions.

Keywords: hyperspectral detection, methane detection, infrared imagine methane detection

1. Introduction

As part of the iDiaGaSys research and development project co-funded by the NCBR, the Gas Transmission Operator GAZ-SYSTEM S.A. and industrial partners, a measurement system was developed for periodic monitoring of leakage and ambient conditions of transmission pipelines. The iDiaGaSys system consists of: the measurement subsystem – a manned helicopter with a mounted imaging Fourier infrared spectroradiometer, and the data analysis subsystem – database infrastructure and diagnostic software with implemented methods of hyperspectral data analysis that enable detection of the presence of methane and prohibited objects in the gas pipeline environment [1].

The Fourier imaging infrared spectroradiometer miniHyper-Cam Airborne, was mounted on a Robinson R44 helicopter using stabilised platform suspended from a GSS R44 MOUNT (Fig. 1). Paper presents a method for detecting methane emissions using components of a system developed within the iDiaGaSys project and used on a test bench for ground-based measurements.

Fig. 1. Measurement subsystem: Robinson R44 helicopter with mounted imaging Fourier infrared spectroradiometer
Rys. 1. System pomiarowy: helikopter Robinson R44 z zamontowanym obrazowym fourierowskim spektroradiometrem podczerwieni

Autor korespondujący:
Mariusz Kastek, mariusz.kastek@wat.edu.pl

Artykuł recenzowany
nadesłany 11.07.2023 r., przyjęty do druku 23.08.2023 r.

2. Experimental Information

2.1. Standoff infrared hyperspectral imaging

he Telops Hyper-Cam is a lightweight and compact hyperspectral imaging instrument that uses Fourier Transform Infrared (FTIR) technology. It features a closed Stirling cycle cooled InAs/InAsSb (SLS) focal plane array (FPA) detector, which contains 320 × 256 pixels over a basic 13.5° × 10.9° field of view (FOV). The spectral resolution is user-selectable from 0.25 cm^{-1} up to 64 cm^{-1} over the entire spectral range of the instrument. The miniHyperCam Airborne was specifically designed for methane investigation. Its optics and detector are specifically tuned on the methane spectral features, 1230–1350 cm^{-1} (7.4–8.2 µm), in the thermal infrared spectral ranges [1].

A method for the detection and quantification of methane emissions based on hyperspectral data from an imaging Fourier infrared spectroradiometer was developed for the project. As part of the project tasks, measurements were carried out under near-real conditions with controlled methane emissions simulating leaks occurring in real conditions on a transmission gas grid. The measurement system was placed at a distance of 50 m from the emission point, for research purposes additionally a blackbody was placed in the field of view of the spectroradiometer, a weather station for monitoring weather conditions and a wind speed variation system. Figure 2 shows photographs of the measurements carried out.

Measurements were carried out for different methane emission volumes, at a constant pressure, which corresponds to the pressure in the transmission pipelines. During the measurements, atmospheric conditions affecting methane detection were monitored: air temperature (22–28 °C), wind speed (0.7–5.7 m/s), atmospheric pressure (998–999 hPa) and relative humidity (51–56 %), emission of the methane on surface. The measurement were done with 8 nm spectral resolution for property detection of the methane cloud. Table 1 provides a summary of the conditions under which the test measurements were carried out.

2.2. Radiative transfer model

It is important to understand that there are many paths that photons can take to arrive at a sensor pointed at the ground. There are photons emitted by materials at their respective temperatures, and transmissions through gasses, as well as absorptions and reflections by opaque objects. Though there are many paths to consider, there are only a few that significantly contribute to the signal measured at the sensor in LWIR measurements. Only those important paths will be considered in this development, which is drawn mainly from the literature focusing on the detection problem, but also from some work done on artificial plume insertion [2–4]. Firstly, a model will be developed for paths that arrive at a sensor which is pointed at the ground, but not viewing any gaseous plumes in the atmosphere. The main contributing paths to the signal in this situation are atmospheric upwelling (L_u), background (ground) radiance (L_g), and noise (L_n). Atmospheric upwelling is radiance that comes from the atmosphere's thermal emission at its temperature. The ground radiance is described as a combination of the thermal emission of an object at the ground's temperature scaled by the emissivity of the material emitting (ε_g), and atmospheric downwelling. The noise term encompasses a few effects including the noise on the focal plane and the thermal emission of the sensor itself onto its focal plane. The combination measured at the sensor can be stated as:

$$L_{clear}\left(\lambda\right) = L_u\left(\lambda\right) + L_g\left(\lambda\right)\tau_{atm}\left(\lambda\right) + L_n\left(\lambda\right) \quad (1)$$

which describes the attenuation of the ground radiance by the transmissivity of the atmosphere, τ_{atm}. This also denotes the wavelength $\left(\lambda\right)$ dependence of all these terms. The background radiance must be further broken up into constituent terms:

$$L_g\left(\lambda\right) = B\left(\lambda, T_g\right)\varepsilon_g\left(\lambda\right) + L_d\left(\lambda\right)\left[1-\varepsilon_g\left(\lambda\right)\right] \quad (2)$$

The background material is held to be at some temperature T_g, and it is assumed to be radiating as a perfect blackbody

Fig. 2. Measurement stand for simulating methane emissions (1 – point of controlled emission of the methane, 2 – weather station, 3 – blackbody) and miniHC Airborne measurement system during measurements
Rys. 2. Stanowisko pomiarowe do symulacji emisji metanu (1 – punkt kontrolowanej emisji metanu, 2 – stacja meteorologiczna, 3 – ciało doskonale czarne) i miniHC Airborne system podczas pomiarów

Table 1. Test conditions for the detection of methane emissions
Tabela 1. Warunki pomiarowe podczas wykrywania emisji metanu

No.	Number of measurements	Pressure of methane (bar)	Emission volumes (l/min)	Wind speed (m/s)
1	150	20.2	5	0.7–4.6
2	141	20.2	7	0.7–4.7
3	110	20.2	10	0.7–5.6
4	61	20.2	15	0.7–5.6
5	31	20.2	30	0.2–5.7
7	35	20.2	40	0.3–5.4

does. The $B(\lambda, T_g)$ function represents the Planck function for radiating blackbodies. This radiation is scaled by the emissivity of the material, ε_g. The other significant contribution to the background radiance term is the reflected atmospheric downwelling. The atmosphere, as previously mentioned, radiates upwards towards the sensor, but some of that energy will be radiated towards the ground and consequently reflected back towards the sensor. This radiance will not be perfectly reflected, as some will be absorbed by the material. However, for simplicity's sake, it is assumed that the particles absorbing this downwelled radiance are in local thermodynamic equilibrium [5, 6].

Including the effects of a plume in scene can be done in a few short steps. The paths that govern this model are slightly more complicated than before. The atmospheric upwelling radiance remains a significant contributor to the signal, but the downwelling radiance that is reflected to the sensor now passes through the plume. The plume has a similar effect on the background thermal radiance. The resultant effect on these signals (reflected downwelling and background thermal radiance) is further attenuation based on the transmission of the plume (τ_p). The radiance of the plume material itself also contributes to the signal model. This radiance (L_p) occurs at the temperature of the plume material, and must pass through (and thus be attenuated by) the intervening atmosphere to reach the sensor. The atmospheric attenuation is assumed applied to the plume at the same strength it is applied to the background thermal radiance path. This is because the plume is assumed to be close to the ground, rather than much closer to the sensor. The result of these effects can be written as:

$$L_{plume}(\lambda) = L_u(\lambda) + L_g(\lambda)\tau_{atm}(\lambda)\tau_p(\lambda) + \\ + L_p(\lambda)\tau_{atm}(\lambda) + L_p(\lambda) \tag{3}$$

This statement describes many of the important paths and their terms, but what is desired is to express this model with a signal term (and an associated strength) and an additive noise term. The signal term should also be a function of the signature of the chemical being detected, $b(\lambda)$. The linear expression from this model that explicitly involves $b(\lambda)$. The transmission of the plume can be expressed as follows:

$$\tau_p(\lambda) = \exp(-cb(\lambda)) \approx 1 - cb(\lambda), \tag{4}$$

where c is the column density of the gas plume as a measure of the amount of intervening matter between an sensor and the background observed, and the chemical signature of the gas is $b(\lambda)$ [10]. This transmissivity is approximately linearized using the assumption that $cb(\lambda)$ is small. The assumption of a small $cb(\lambda)$ must be kept true, otherwise the linear model will be unfaithful to the physical process.

2.3. Method for the detection and quantification of methane emissions

The developed method for detection and quantification methane emissions was based on hyperspectral data analysis using various techniques including spectral unmixing, gas detection algorithms and statistics method. Developed method is doing the analysis hyperspectral data following steps:

- Collected hyperspectral data: Hyperspectral data can be collected using miniHyperCam Airborne. The data were collected in special stand with full control emission.
- Preprocessing: Preprocessing involves removing noise, atmospheric corrections, data normalization and data calibration. Atmospheric corrections is very important for methane detection since the presence of methane can affect the atmospheric transmission in the far-infrared region. In the method was used one of the atmospheric correction methods, such as the atmospheric radiative transfer (ART) model.
- Methane emission detection: Gas detection algorithm is used to identify the presence of methane in hyperspectral data. The algorithm is used spectral signatures of methane to identify methane absorption bands based on adaptive matched filter (AMF), which identifies the methane absorption feature. In the method was used a combination of clutter matched filter CMF and SAM, with appropriate thresholding and spatial filtering, to detect. The PNNL infrared database is used as a reference library for spectral characteristic of the methane [4, 7–9].
- Methane emission: Algorithm of the gas quantification involves estimating the concentration of the gas from its spectral characteristic pixels with positive detection results. The concentration can be estimated using various methods such as the Beer-Lambert law, which function of the surface thermodynamic temperature while transmittance is function of gas concentration (expressed in ppm), path length l (expressed in meters) and the gas molar absorptivity κ (with units of $m^{-1}\cdot ppm^{-1}$) as expressed in (4) [5].

In addition, a module has been implemented to convert the concentration of a gas expressed in (ppm·m) to (g/s). Derived from the equation of state of a perfect gas (Clapeyron's equation) is the equation of state describing the relationship between temperature, pressure and volume of a perfect gas, which can be expressed by the formula:

$$pV = nRT, \tag{5}$$

where p is the pressure of the gas (in Pa), V is the volume occupied by the gas (in m^3), T is the temperature of the gas (in Kelvin, K), R is the gas constant (equal to 8.314462618 J K^{-1} mol^{-1}), n is the number of moles of particles in the gas.

The molar volume is the volume occupied by one mole of a substance and is given by the formula:

$$V_m = \frac{V}{n} = \frac{M}{\rho} = \frac{M \cdot V}{m}, \tag{6}$$

where: V_m – molar volume (unit: m^3/mol), V – volume of n moles of substance, M – molar mass (unit: kg/mol), m – mass of substance (unit: kg), ρ – density (unit: kg/m^3).

From equation (5), the molar volume can be determined according to the formula:

$$V_m = \frac{V}{n} = \frac{RT}{p}. \tag{7}$$

Knowing the volume of the mixture V_x, the molar volume V_m of the substance and its concentration value S_{ppm} given in ppm, the number of moles of the substance can be determined using the formula:

$$n = \frac{S_{ppm} \cdot 10^{-6} \cdot V_x}{V_m}. \tag{8}$$

Based on formulae (6) and (8), the formula for the mass of the substance can be derived:

$$m = \frac{S_{ppm} \cdot V_x \cdot M}{V_m} \cdot 10^{-6}. \tag{9}$$

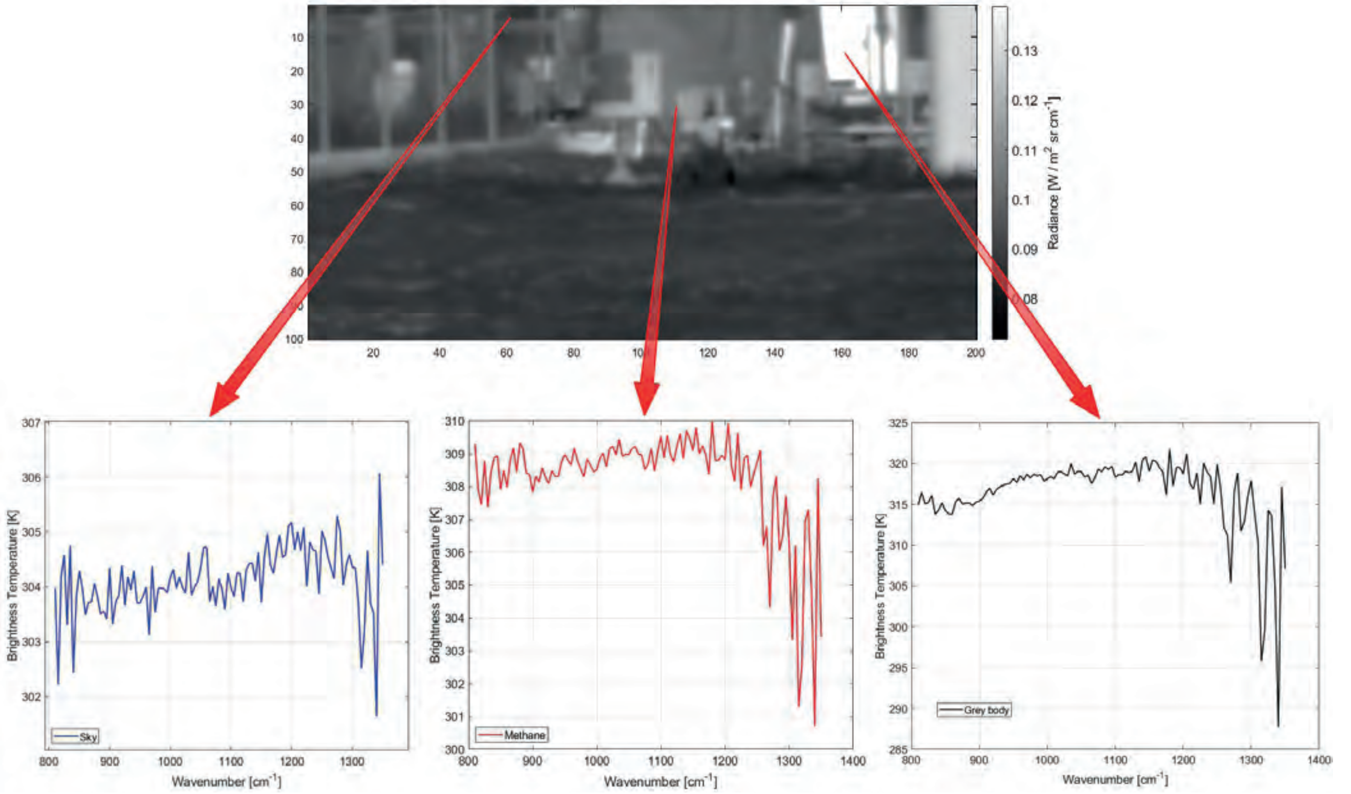

Fig. 3. Example of data registered by miniHyperCam Airborne
Rys. 3. Przykładowe wyniki otrzymane podczas popmiarów za pomocą miniHyperCam Airborne

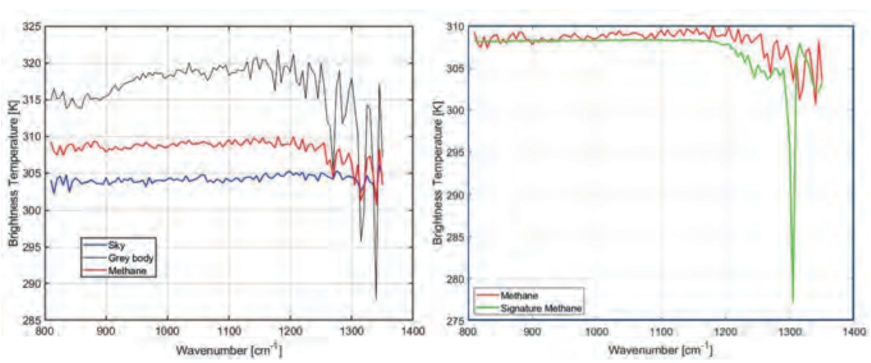

Fig. 4. Infrared spectra associated with a single pixel representative of sky radiance (Sky), the wall of the house (Grey Body) and methane emission point (Methane) (left). The spectra are plotted as a brightness temperature scale for clarity purposes. The radiance methane emission point (Methane) and radiance methane spectral from NIST library (Signature Methane) [9] are shown (right) for comparison purposes. Presented brightness temperature is a measurement of the radiance traveling from source to the sensor, expressed in units of the temperature of an equivalent black body, it is better present the spectral characteristic
Rys. 4. Widma w podczerwieni dla pojedynczych pikseli: nieba (Sky), ściany domu (Grey Body) i punktu emisji metanu (Methane) (po lewej). (Metan) (po lewej). Widma są wykreślone jako rozkład temperatury w celu lepszego zaprezentowania ich zmian. Radiancja punktu emisji metanu (Metan) i widmo promieniowania metanu z biblioteki NIST z biblioteki NIST (Signature Methane) [9] (po prawej) została przedstawiona w celu ich porównania. Przedstawiona temperatura jest wynikiem pomiaru radiancji od źródła do systemu pomiarowego, wyrażona w jednostkach temperatury równoważnej dla ciała czarnego, w taki sposób jest lepiej jest przedstawić charakterystykę widmową

Inserting into equation (9) the molar volume determined according to equation (7), we obtain:

$$m = \frac{S_{ppm} \cdot V_x \cdot M \cdot p}{RT} \cdot 10^{-6}. \qquad (10)$$

When the concentration value of the substance S_{ppm-m} is given in ppm-m, and knowing the areas of the mixture A_x, formula (10) for the mass of the substance can be written in the form:

$$m = \frac{S_{ppm-m} \cdot A_x \cdot M \cdot p}{RT} \cdot 10^{-6}. \qquad (11)$$

A concentration map, which is the instantaneous state of the gas cloud, is then calculated through a gas flow rate conversion module that calculates the amount of gas transported by the wind in one second. Its shape and concentration depend on the flow rate and wind speed. Assuming that the wind direction will be orthogonal to the spectroradiometer's direction of view, the flow rate can be calculated as the product of the wind speed and a 1 m 'slice' of the methane cloud.

$$f = m_{gas_{1m}} s_{wind} \qquad (12)$$

where: – emission [g/s], $m_{gas_{1m}}$ – mass of gas in a 1 m wide cloud; s_{wind} – wind speed (unit m/sec) in the direction perpendicular to the direction of spectroradiometer observation.

The various computational modules were implemented in the MATLAB environment and used to analyze hyperspectral data for the detection and quantification of methane emissions during the ongoing test studies.

Table 2. Data prepared for analysis after detection of methane emissions
Tabela 2. Wyniki otrzymane po przeprowadzonych analizach emisji metanu

File name	Total measured methane emission	Wind speed	Total methane emission after wind correction	Set up methane emission from pipeline
	(l/min)	(m/s)	(l/min)	(l/min)
Test_16_20220810_114800_694.sc	3.308	3.6	11.907	15
Test_16_20220810_114801_827.sc	3.593	3.6	12.934	15
Test_12_20220810_112654_167.sc	2.48	3.9	9.69	10
Test_12_20220810_112655_300.sc	1.65	3.9	6.44	10
Test_7_20220810_111343_156.sc	2.238	3.8	8.505	7
Test_7_20220810_111344_295.sc	1.711	3.8	6.502	7
Test_1_20220810_104516_950.sc	1.478	1.9	2.809	5
Test_1_20220810_104518_085.sc	2.912	1.9	5.533	5

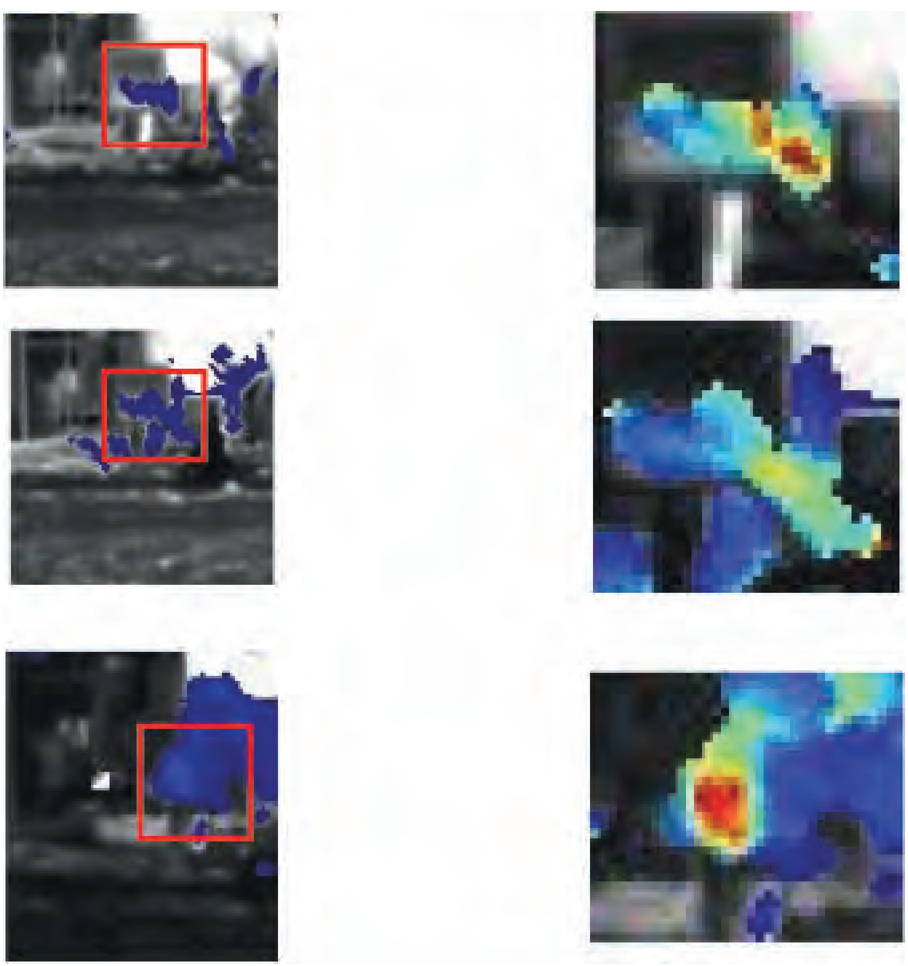

Fig. 5. Column density map of methane set up emission from pipeline: a) 7 l/min, b) 10 l/min, c) 30 l/min. Left side pictures shows the image recoded by miniHyperCam Airborne with the column density map of the methane without analysis of the emission, right side it is zooming the point of the emission methane, the color present the emission of the methane
Rys. 5. Przykładowe rozkłady emisji metanu zarejestrowane podczas pomiarów emisji: a) 7 l/min, b) 10 l/min, c) 30 l/min. Obrazy po lewej stronie przedstawiają rejestracje wykonane za pomocą miniHyperCam Airborne z mapą wykrytej chmury metanu, obrazy po lewej stronie to wybrany fragment obrazu w wynikiem z chmurą matanu przedstawiającą rozkład stężenia metanu będącym wynikiem przeprowadzonej analizy

3. Results of the test studies

3.1. Hyperspectral data and analysis results

Many materials encountered in outdoor environments behave like infrared grey bodies, i.e. are featureless across all wavelengths. Unlike many common materials, gases like methane (CH_4) and water vapor (H_2O) behave like selective absorbers/emitters of infrared radiation. Their absorption/emission pattern is function of wavelength (or wavenumbers).

The recorded measurement data at the measuring station according to the measurement plan (part 2.1) were analysed, and an analysis of the results obtained is presented below. Therefore, their presence can be easily detected when looking at high spectral resolution infrared data. Hyperspectral imaging allows recording of such spectra for each pixel. In order to illustrate the great variety of infrared-active material within a scene, typical spectra associated with selected pixels are shown in Fig. 3.

Table 3. Validation of the detection method for methane emissions in the sensitivity range
Tabela 3. Walidacja metody detekcji emisji metanu w zakresie czułości metody

Emissions analysed (l/min)	Number of measurements	Number of measurements with methane detection	Sensitivity of the method – probability of detecting emissions (%)
5.0	150	91	60.7
7.0	141	135	95.7
10.0	110	110	100
15.0	61	61	100
30.0	31	31	100
40.0	35	35	100

The infrared spectrum associated with a grey body surface should be a straight curve. However, because of the presence of atmospheric gases in the path located between the infrared sensor and the target, the measured spectrum is highly structured. They are mostly associated with ground-level atmospheric component like water vapor, CH_4 and nitrous oxide (N_2O) (Fig. 4). Since the atmospheric water content is typically a few orders of magnitude higher than the other components, water spectral features are dominant. The high-resolution infrared spectra corresponding to a pixel close to the drill is quite different and shares many similarities with the methane reference absorption spectrum.

3.2. Methane column density maps

Based on the recorded data for the different measurement conditions (Table 1), the hyperspectral data were processed and recalculated according to the adopted method. As results, maps of the distribution of detected methane were obtained, which for visualisation purposes were presented as a fusion of a thermogram (broadband image) and a pixel map with detected methane. Example results are presented in the images for different emissions in Fig. 5.

The results data for each of the files corresponding to the measurement of methane emissions was then performed to assess the effectiveness of the method for detecting and quantifying methane emissions. Example data for analysis are shown in Table 2.

3.3. Analysis of the results obtained for the evaluation of the correctness of methane detection

The capability of the system under development to detect and measure methane emissions from the transmission gas grid was assessed on the basis of test studies for controlled methane emission rates ranging 5–40 l/min. A total of approximately 520 tests were performed, which formed the basis for the validation of the qualitative method for detecting methane emissions (Table 1).

During the validation, parameters such as sensitivity, limit of detection, specificity and accuracy were taken into account. From the point of view of the validation of a qualitative method for the detection of methane emissions, the most important validation parameter is the sensitivity of the method, which in this case means the ability of the method to detect the emissions actually occurring. The acceptance criterion for method sensitivity was a 50 % probability of detecting methane emissions at 7 l/min, which increases linearly to 90 % at emissions of 150 l/min. The results of the sensitivity assessment of the method for detecting methane emissions are shown in Table 3.

The results obtained during the validation of the methane emission detection method in terms of its sensitivity meet the established acceptance criteria, confirming the suitability of the method for detecting fugitive methane emissions from the transmission gas grid.

A similar parameter to the sensitivity of the method is the lower detection limit, which in this case means the smallest amount of methane emissions that can be detected by the method with a given probability. Given that the method under development is a field and screening method, it was assumed that the lower limit of detection is 7.0 l/min. It is the emission level for which the sensitivity of the method is greater than or equal to 50 %.

Based on the test results shown in Table 3, it can be concluded that the developed method meets the established acceptance criteria, as it has a detection limit below 5.0 l/min.

Another validation parameter of the qualitative method is specificity. Methods that are characterized by high specificity generate a small number of so-called 'false alarms', in this case involving the detection of a leak when there is no leak. Because of the actions to be taken by the gas grid operator after a leak has been detected, it was assumed that the specificity of the method should not be lower than 90%, meaning that the validated method would generate no more than 10 % false alarms. During the conducted tests, there were no false detections of methane emissions, the hypothesis that the developed method is 100 % specific needs to be confirmed under more diverse field conditions.

The last of the validated parameters of the qualitative method for detecting methane emissions was accuracy. In quantitative methods, this is the parameter that combines the sensitivity and specificity of the method:

$$AC = \frac{SP + SN}{N_+ + N_-} \cdot 100\% \tag{13}$$

where $\frac{SP}{N_+}$ is a sensitivity and $\frac{SN}{N_-}$ is a specificity, where SP – a number of positive tests assessed as positive, SN – a number of negative tests assessed as negative, N_+ – the total number of positive tests performed and N_- – is the total number of negative tests performed.

Taking into account the field nature of the method and formula (13) with the acceptance criteria for sensitivity (above 50 %) and specificity of the method (above 90 %), the acceptable accuracy of the method was assumed to be 70 %. This means that 7 out of 10 results obtained with the validated method will be evaluated correctly with respect to the true value. The field results obtained indicate 100 % specificity of the method and therefore the determined accuracy of the method will be the same as its sensitivity. Based on the results collected in Table 2, it can be concluded that the validated method has acceptable accuracy for methane emissions above 7.0 l/min.

4. Conclusion

The development of a remote system for detecting and measuring methane emissions from the transmission gas grid is a major challenge due to the size of the area to be monitored, the range of methane emissions and changing weather conditions during the measurements. The measurement subsystem developed as part of the iDiaGaSys project is designed to detect and measure methane emissions from the transmission gas grid using the FTIR technique. The Fourier imaging infrared spectroradiometer mini-HyperCam Airborne selected for this purpose together with the developed computational algorithms successfully passed initial tests in the field of detecting methane fugitive emissions greater than 5 l/min. Due to the method of conducting the initial tests (stationary tests from the ground), in order to fully assess the suitability of the developed measurement subsystem, it is required to perform tests in real measurement conditions.

Acknowledgements

The authors inform that the presented system concept and its implementation has been co-financed by the European Union from the European Regional Development Fund under the Intelligent Development Programme and the Gas Transmission Operator GAZ-SYSTEM Joint Stock Company. The project was implemented under the competition of the National Centre for Research and Development: 4/4.1.1/2019 as part of the INGA Joint Undertaking.

The photos in the article are not related to the infrastructure operated by GAZ-SYSTEM.

Bibliografia

1. Timofiejczuk A., Rzydzik S., Holewa-Rataj J., Kukulska-Zając E., Kastek M., Pawelski D., Brawata S., Gawełda B., *The concept of a system for monitoring the condition of gas transmission pipelines and their surroundings*, “Nafta-Gaz”, Vol. 79, No. 1, 2023, 52–60, DOI: 10.18668/NG.2023.01.06.
2. Lashof D.A., Ahuja D.R., *Relative Contributions of Greenhouse Gas Emissions to Global Warming*, “Nature”, Vol. 344, 1990, 529–531, 1990.
3. Tremblay P., Savary S., Rolland M., Villemaire A., Chamberland M., Farley V., Brault L., Giroux J., Allard J.-L., Dupuis E., Padia T., *Standoff gas identification and quantification from turbulent stack plumes with an imaging Fourier-transform spectrometer*, Proceedings of SPIE, Vol. 7673, 2010, DOI: 10.1117/12.850127.
4. Gålfalk M., Olofsson G., Crill P., Bastviken D., *Making methane visible*, “Nature Climate Change”, Vol. 6, 2016, 426–430.
5. Moritz A., Hélie J.-F., Pinti D.L., Larocque M., Barnetche D., Retailleau S., Lefebvre R., Gélinas Y., *Methane baseline concentrations and sources in shallow aquifers from the shale gas-prone region of the St. Lawrence lowlands*, “Environmental Science and Technology”, Vol. 49, No. 7, 2015, 4765–4771, DOI: 10.1021/acs.est.5b00443.
6. Kastek M., Piątkowski T., Dulski R., Chamberland M., Lagueux P., Farley V., *Hyperspectral Imaging Infrared Sensor Used for Chemical Agent Detection and Identification*, 2012 Symposium on Photonics and Optoelectronics, DOI: 10.1109/SOPO.2012.6270545.
7. Coleman T.F., Li Y., *An Interior Trust Region Approach for Nonlinear Minimization Subject to Bounds*, “SIAM Journal on Optimization”, Vol. 6, No. 2, 1996, DOI: 10.1137/0806023.
8. Farley V., Chamberland M., Lagueux P., Vallières A., Villemaire A., Giroux J., *Chemical agent detection and identification with a hyperspectral imaging infrared sensor*. Proceedings of SPIE, Vol. 6739, 2007, DOI: 10.1117/12.736864.
9. Kastek M., Piątkowski T., Trzaskawka P., *Infrared imaging Fourier transform spectrometer as the stand-off gas detection systems*, “Metrology and Measurement Systems”, Vol. XVIII, No. 4, 2011, 607–620, DOI: 10.2478/v10178-011-0058-4.

Inne źródła

10. https://webbook.nist.gov/cgi/cbook.cgi?ID=C74828&Type=IR-SPEC&Index=1

Zdalne wykrywanie i kwantyfikacja emisji metanu na podstawie analizy danych hiperspektralnych

Streszczenie: Pomiar emisji metanu z wycieków występujących na rozległej terytorialnie sieci gazociągów przesyłowych jest zagadnieniem aktualnym i wysoce pożądanym z punktu widzenia bezpieczeństwa i ograniczenia emisji metanu do atmosfery. Zdalna detekcja metanu jest problem, którego rozwiązanie techniczne opiera się na kilku typach urządzeń optoelektronicznych, np. kamerach termowizyjnych z zestawami filtrów optycznych kamery termowizyjne z zestawami filtrów optycznych, spektroradiometry, systemy laserowe DIAL (DIfferential Absorption Lidar). Z drugiej strony, kwantyfikacja wielkości emisji jest w większości przypadków realizowana przez systemy spektroradiometryczne. W niniejszym artykule zostanie przedstawiona metoda analizy danych hiperspektralnych z obrazującwego fourierowskiego spektroradiometru podczerwieni. Pomiary zostały wykonane na specjalnie zbudowanym stanowisku symulującym emisję metanu z sieci przesyłowej. Dane uzyskane z poziomu gruntu w różnych warunkach atmosferycznych, wraz z wynikami ich analizy dla różnych emisji metanu.

Słowa kluczowe: hiperspektralna detekcja w podczerwieni, detekcja metanu, obrazowa detekcja metanu w podczerwieni

Mariusz Kastek, PhD, Eng.

mariusz.kastek@wat.edu.pl
ORCID: 0000-0001-7184-5228

A graduate of the Electronics Department of the Military University of Technology (1993). Since 1997, he has been an employee of the Military University of Technology. He obtained the title of doctor of technical sciences in 2002. He deals with the problems of object detection in infrared systems, as well as signal analysis and detection algorithms implemented in infrared devices. Author and co-author of over 70 publications. He works as an assistant professor at the Institute of Optoelectronics of the Military University of Technology.

Andrzej Ligienza, MSc, Eng.

andrzej.ligienza@wat.edu.pl
ORCID: 0000-0002-5789-8531

Andrzej Ligienza graduated BSc in the Military University of Technology (2014) at the Faculty of Mechatronics with a specialty of ISM. MSc graduated in 2016 at the faculty of Electronics. Currently PhD candidate and assistant lecturer at Faculty of Optoelectronics..

Tomasz Sosnowski, PhD, Eng.

tsosnowski@wat.edu.pl
ORCID: 0000-0003-4082-8366

Absolwent Wydziału Elektroniki Wojskowej Akademii Technicznej (1993). Tytuł doktora nauk technicznych uzyskał w 2003 r. Zajmuje się problematyką związaną z projektowaniem i programowaniem systemów cyfrowych, cyfrową analizą sygnału, analizą obrazu termograficznego, a także zastosowaniem układów mikroprocesorowych i programowalnych w technice podczerwieni.

Jadwiga Holewa-Rataj, MSc

holewa@inig.pl
ORCID: 0000-0001-8928-6081

A graduate of environmental protection at the Jagiellonian University (2006). Since 2006, he has been an employee of the Oil and Gas Institute - National Research Institute. In her professional work, she deals with issues related to environmental protection in the oil and gas industry, including, among others, methane emission measurements and inventory. She is a co-author of over 25 publications in national journals and about 30 speeches at scientific and technical conferences.

Mateusz Rataj, MSc, Eng.

rataj@inig.pl
ORCID: 0000-0003-2335-6221

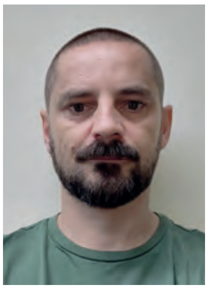

A graduate of the Fuels and Energy Faculty the AGH University of Science and Technology in Kraków (2008), majoring in Fuel Technology. Since 2008, an employee of the Oil and Gas Institute - National Research Institute in the Laboratory for Testing Gas and Heating Devices. As part of his professional activity, he deals with the problems of emission of pollutants into the atmosphere, thermovision and the development of new technologies.

Prof. Anna Timofiejczuk, DSc, PhD, Eng.

anna.timofiejczuk@polsl.pl
ORCID: 0000-0003-2941-4955

Dean of the Faculty of Mechanical Engineering at the Silesian University of Technology. The area of scientific interest is technical diagnostics, signal and image analysis, applications of artificial intelligence and Industry 4.0. In 2018, together with her team, she created the first competence center for Industry 4.0 in Poland. In 2015, she developed a dual studies program, and is also the initiator and organizer of the Edual conference - dual education for Industry 4.0. She was a member of the Consulting Team of the Future Industry Platform of the Ministry of Entrepreneurship and Technology. He is a member of the Automotive Council, including electromobility in the Ministry of Industry and Development. Prof. Anna Timofiejczuk is a coordinator Priority Research Area – Process Automation and Industry 4.0, and she is also the deputy director of Industry 4.0 Center of Silesian University of Technology.

Sebatian Rzydzik, PhD

sebastian.rzydzik@polsl.pl
ORCID: 0000-0003-3352-3986

An assistant professor at the Department of Fundamentals of Machine Design at the Silesian University of Technology. He is interested in broadly understood mechatronics, mobile robotics (land and air), software development (including simulation), signal processing techniques and the design of mechanical systems. He cooperated with various companies in the field of research and development works and worked as an IT engineer and mechanical engineer. Author or co-author of over 50 publications in the field of robotics, technical diagnostics, design of mechanical systems, artificial intelligence, including advisory systems.